

Geophysical limits to global wind power

Kate Marvel^{1*}, Ben Kravitz² and Ken Caldeira²

There is enough power in Earth's winds to be a primary source of near-zero-emission electric power as the global economy continues to grow through the twenty-first century. Historically, wind turbines are placed on Earth's surface, but high-altitude winds are usually steadier and faster than near-surface winds, resulting in higher average power densities¹. Here, we use a climate model to estimate the amount of power that can be extracted from both surface and high-altitude winds, considering only geophysical limits. We find wind turbines placed on Earth's surface could extract kinetic energy at a rate of at least 400 TW, whereas high-altitude wind power could extract more than 1,800 TW. At these high rates of extraction, there are pronounced climatic consequences. However, we find that at the level of present global primary power demand (~18 TW; ref. 2), uniformly distributed wind turbines are unlikely to substantially affect the Earth's climate. It is likely that wind power growth will be limited by economic or environmental factors, not global geophysical limits.

Here, we quantify geophysical limits to wind power by applying additional drag forces that remove momentum from the atmosphere in a global climate model. We perform simulations in which drag is applied to either the near-surface environment or the entire atmosphere, and analyse consequences for the atmospheric kinetic energy budget and climate. When small amounts of additional drag are added to the atmosphere, the rate of kinetic energy extraction (KEE) increases. However, in the limit of infinite drag, the atmosphere is motionless and there is no kinetic energy to extract. This suggests that there must be some amount of added drag that maximizes KEE. We refer to this maximum KEE as the geophysical limit to global wind power. Here, we consider only geophysical limitations, not technical or economic constraints on wind power.

The large-scale climate impacts of increased surface drag have been considered in previous studies. In an idealized global climate model, surface friction was uniformly increased across the globe, and this was found to decrease atmospheric kinetic energy and shift eddy-driven mid-latitude jets polewards³. In a general circulation model with specified sea surface temperatures, altered surface drag and modified surface roughness height over selected regions, caused slight increases in global surface temperatures⁴. This effect was also observed when land-surface roughness was increased in a climate model incorporating a mixed-layer ocean⁵. Other studies have investigated the wind anomaly patterns produced by isolated regions of increased surface roughness⁶; and estimated wind resource potential over land that was not ice-covered⁷. However, these studies focused solely on increased surface drag. The effects of increased drag in the interior of the atmosphere have been studied⁸ where a drag term was added to regions of the atmosphere where wind speeds exceeded a cutoff velocity. Unfortunately, aspects of that work make their results difficult to interpret. For example, they include wake turbulence in a term that involves momentum transfer to the turbine blades despite the fact that there is no such momentum transfer in the wake and

introduce a frictional parameter with units that are difficult to reconcile with their equations.

Results

Limits on wind power availability. We differentiate among three types of kinetic energy loss represented in the CAM3.5 model⁹:

- Viscous dissipation refers to the rate at which work is done by viscosity of air in converting mean and turbulent kinetic energy to internal energy through heat.
- Roughness dissipation refers to the rate at which pre-existing surface momentum sinks such as the land or ocean surface dissipate kinetic energy.
- KEE refers to the removal of kinetic energy caused by momentum loss to the added momentum sinks. In the case of wind turbines, the kinetic energy would be converted to mechanical or electrical energy, most of which would ultimately be dissipated as heat. In our simulations, this heat is dissipated locally. Drag added to the atmosphere has important secondary consequences: the velocity change and associated velocity gradients may affect both roughness and viscous dissipation. Here, KEE refers only to the rate of transfer of kinetic energy to added momentum sinks.

The parameter we introduce to vary additional drag is ρ_{Area} : the effective extraction area per unit volume, discussed in Methods and Supplementary Section SA.1. Figure 1a shows KEE as a function of ρ_{Area} for cases where drag has been added to the near-surface layers (cases labelled SL(n)) and whole atmosphere (cases labelled WA(n)). (See also Supplementary Fig. SA.1a for the results on logarithmic scales.) As expected for low values of added drag, increasing extraction area increases KEE, that is, $(d(\text{KEE})/d\rho_{\text{Area}}) > 0$. At the geophysical limit to global wind power, $(d(\text{KEE})/d\rho_{\text{Area}}) = 0$. As shown in Fig. 1b, for both the near-surface and whole-atmosphere cases we approach but do not reach this limit. Therefore, the geophysical limits exceed the maximum KEE values found in our study for both cases.

Figure 1b shows the depletion of atmospheric kinetic energy as a function of KEE. We find that for every additional watt dissipated by drag added in the near-surface cases, total atmospheric kinetic energy decreases by 80 kJ, whereas each additional watt dissipated in the whole-atmosphere cases decreases atmospheric kinetic energy by 400 kJ.

From Fig. 1a,b we can infer that the geophysical limit on wind power availability is greater than 428 TW in the surface-only cases, and greater than 1,873 TW in the whole-atmosphere cases. These lower bounds on geophysical limits on airborne wind power exceed the present global primary energy demand of 18 TW by factors greater than 20 and 100, respectively. The results from all cases are summarized in Supplementary Table SA1.

Kinetic energy production and the atmospheric heat engine.

In steady state, net kinetic energy dissipation is balanced by net kinetic energy production. Furthermore, in the atmosphere, kinetic energy is produced by conversion of available potential

¹Program for Climate Model Diagnosis and Intercomparison, Lawrence Livermore National Laboratory, PO Box 808, L-103 Livermore, California 94551, USA, ²Carnegie Institution Department of Global Ecology, 260 Panama Street, Stanford, California 94305, USA. *e-mail: marvel1@llnl.gov.

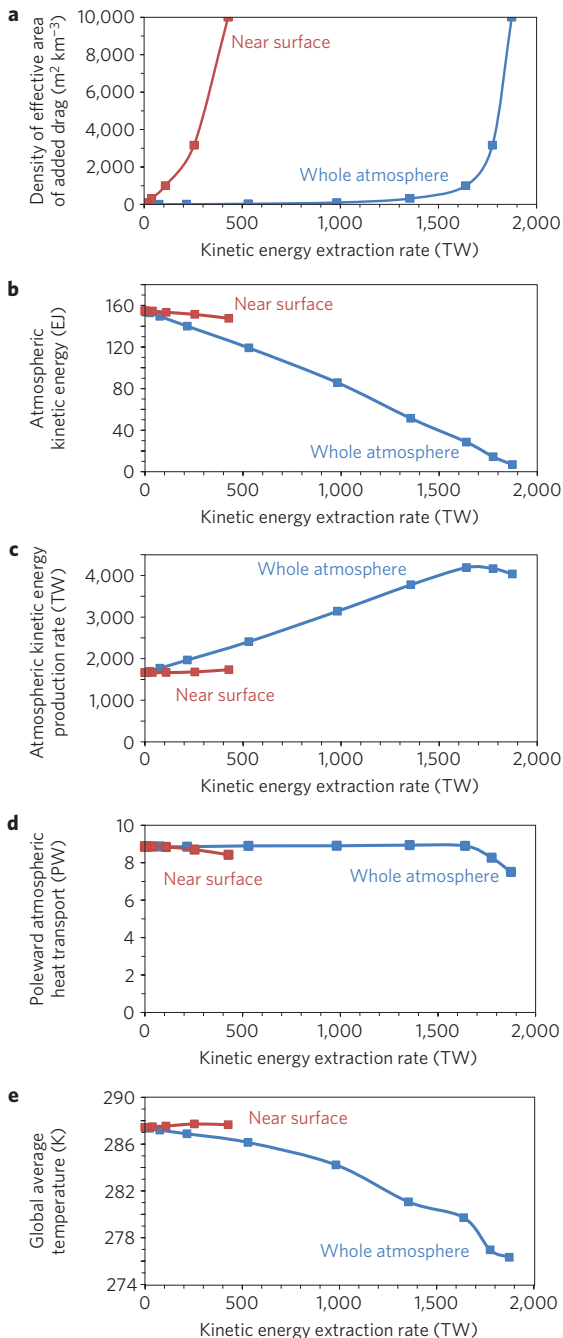


Figure 1 | Global results for climate model simulations with drag added near the surface and throughout the whole atmosphere. The horizontal axis for all panels is the global total amount of KEE. **a**, Areal density of effective drag added needed to produce the specified amount of global total KEE. **b**, Atmospheric kinetic energy decreases nearly linearly with KEE. **c**, The production rate of atmospheric kinetic energy is relatively insensitive to added surface drag but increases by about 0.8 W for each watt of KEE. **d**, Total poleward atmospheric heat transport is not markedly affected by added drag, except when very large amounts of drag are added to the atmosphere in the whole-atmosphere cases. **e**, Global average temperature decreases markedly in the whole-atmosphere cases.

energy. Therefore, sustained increases in net dissipation imply increases in net production of available potential energy and conversion to kinetic energy.

Figure 1c shows the total rate of dissipation (the sum of viscous dissipation, roughness dissipation and KEE) as a function of KEE.

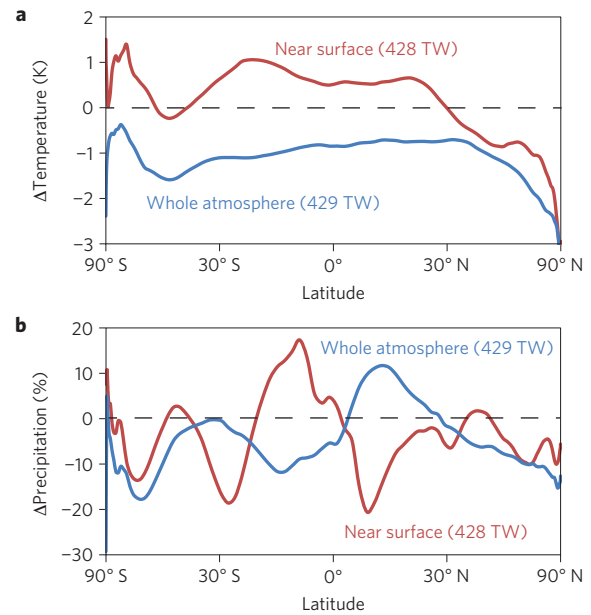


Figure 2 | Zonal mean departures for cases extracting 428–429 TW from atmospheric winds, expressed as departures from zonal mean values in the control case. The red lines are for the SL(5) case with an effective areal density of added drag of $10^4 \text{ m}^2 \text{ km}^{-3}$. The blue lines are for the WA(7.63) case with an effective areal density of added drag of $24.3 \text{ m}^2 \text{ km}^{-3}$. **a**, Temperature departures in K. **b**, Precipitation departures as a percentage of control simulation values. These figures represent results for kinetic energy extraction levels that exceed energy demands from civilization by more than a factor of 20.

For the near-surface cases, there is little change in total atmospheric dissipation. However, in the whole-atmosphere cases, for every watt increase of KEE due to added drag cases, total atmospheric kinetic energy production increases by $\sim 0.8 \text{ W}$. The near-linear relationship between added dissipation and total dissipation holds until the KEE in the whole atmosphere exceeds $\sim 1,600 \text{ TW}$. Beyond this value, increases in KEE result in declines in net kinetic energy production.

Figure 1d depicts the net atmospheric energy transport from low latitudes with net atmospheric energy gain to high latitudes with net atmospheric energy loss. To a large extent, atmospheric energy transports must adjust such that energy is transported in steady-state from regions of net energy accumulation to regions of net energy loss. When drag is added near the surface alone, high KEE does cause some decrease in net poleward energy transport. For the whole-atmosphere cases, however, net energy transport remains approximately constant until KEE exceeds $\sim 1,600 \text{ TW}$, after which it declines sharply.

Climate impacts. Figure 1e indicates that uniformly applied surface drag has a slight warming effect, consistent with previous studies^{4,5,10}. However, we find that whole-atmosphere drag can have a large surface cooling effect as KEE approaches the geophysical limit. If we assume that the effects of extracting kinetic energy scale linearly at extraction rates less than 429 TW, then satisfying global energy demand with uniformly distributed wind turbines would cause a global mean temperature increase of 0.03 K for near-surface wind turbines, and a global mean decrease of 0.007 K for turbines distributed throughout the atmosphere.

Figure 2 shows zonal mean temperature change and percentage change in zonal mean precipitation for cases SL(5) and WA(7.63), each of which have approximately the same globally integrated KEE (428 TW and 429 TW, respectively). Zonal mean temperature

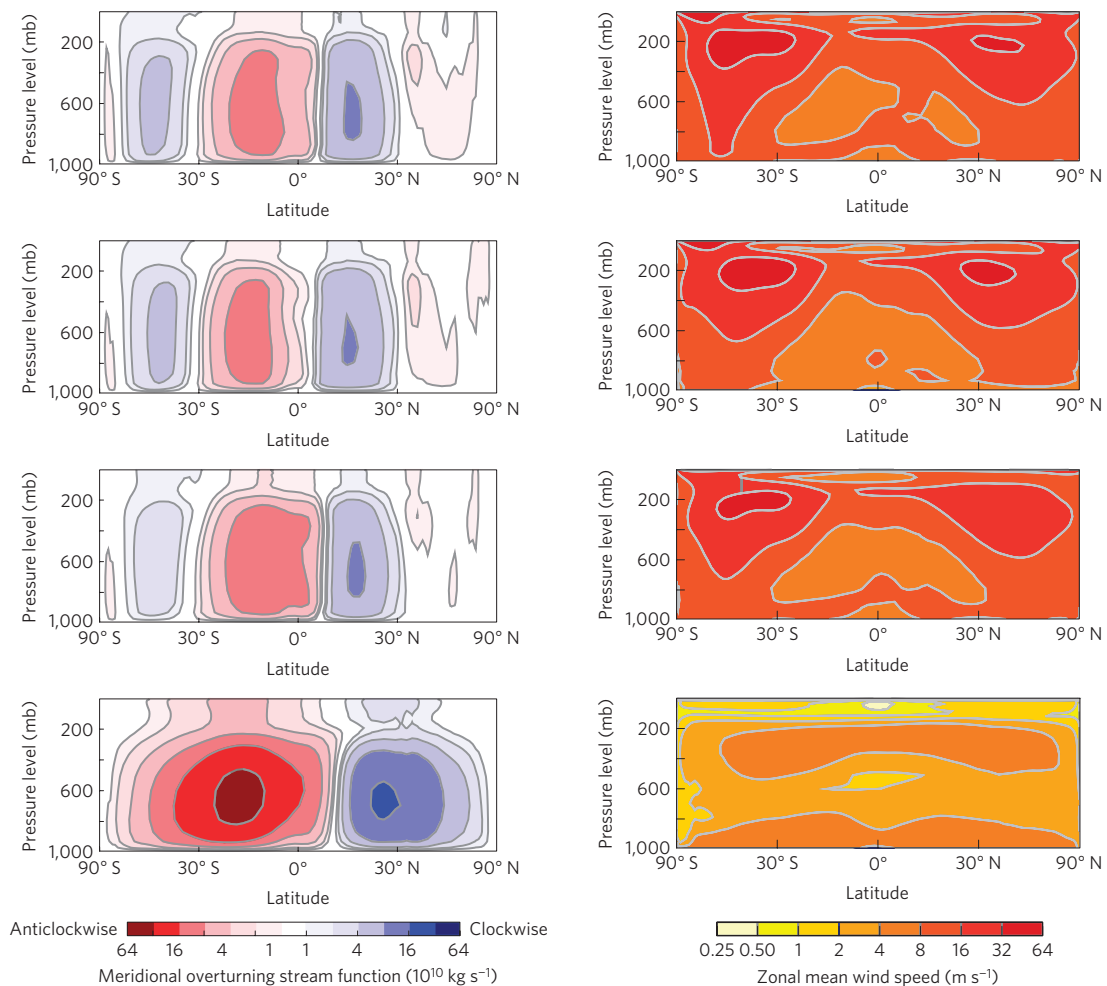


Figure 3 | Circulation changes from large-scale kinetic energy extraction. The left column shows the meridional mass overturning stream function, in $10^{10} \text{ kg m s}^{-1}$ for (from top to bottom) the selected cases, control, SL(5), WA(7.63) and WA(5). Cases SL(5) and WA(5) were chosen because they are our lower-bound estimates of near-surface and whole-atmosphere maximum KEE rates at 428 TW and 1,873 TW, respectively. WA(7.63) was chosen as a whole-atmosphere case that has a similar KEE (429 TW) to the SL(5) case. The right column shows zonal mean wind speeds for (from top to bottom) the control, SL(5), WA(7.63) and WA(5). Cases SL(5) and WA(5) have added drag with areal density $10^4 \text{ m}^2 \text{ km}^{-3}$ in the near-surface and whole atmosphere, respectively. Case WA(7.63) has added drag with areal density $24.3 \text{ m}^2 \text{ km}^{-3}$ in the whole atmosphere.

changes in these cases are of the order of 1 K and percentage changes in zonal mean precipitation are of the order of 10%. This suggests that, at the scale of global energy demand, uniformly distributed wind power would produce zonal mean temperature changes of $\sim 0.1 \text{ K}$ and changes in zonal mean precipitation of $\sim 1\%$ (see Supplementary Section SA2). Thus, reliance on widely distributed wind turbines as an energy source is unlikely to have a substantial climate impact.

Circulation changes. Many quantities shown in Fig. 1 scale nearly linearly with KEE at rates less than $\sim 1,600 \text{ TW}$. Our results suggest that the breakdown of this linear relationship above $\sim 1,600 \text{ TW}$ is due to a regime shift in the atmospheric circulation. Figure 3 shows the meridional overturning stream function for four cases: the control run, SL(5), WA(7.63) and WA(5). SL(5) and WA(5) are chosen because they represent the maximum simulated KEE for near-surface-alone and whole-atmosphere drag, respectively. The meridional overturning stream function for the SL(5) seems similar to that of the control simulation. The stream function for WA(7.63) is less similar, despite the similar amount of KEE. In particular, the downward branches of the Hadley cells shift polewards. In the extreme case of WA(5) the Hadley cells extend to the poles, and poleward heat transport is carried out in each hemisphere by a single

large cell. As discussed in Supplementary Section SA3, similar effects have been observed in numerical and laboratory experiments in which the viscosity of the atmosphere is increased or the Earth's rotation rate is decreased^{11–14}.

The right-hand column of Fig. 3 shows zonal mean wind speed as a function of latitude and pressure. The control case has global mass-weighted average wind speeds of 18.5 m s^{-1} and pronounced mid-latitude jets at around 200 mb. SL(5) shows a similar pattern, with global average wind speeds of 17.9 m s^{-1} , but near-surface winds are reduced by $\sim 30\%$ (see Fig. 1h). Mean wind speeds in WA(7.63) are 15.7 m s^{-1} , and the upper level jets weaken, particularly in the Northern Hemisphere. In the extreme whole-atmosphere case WA(5), mean wind speeds decrease precipitously to 3.1 m s^{-1} .

Discussion and conclusions

In this study, we establish lower bounds on the maximum rate at which kinetic energy may be extracted from the atmosphere by added momentum sinks. Using a climate model, we simulate this extraction by adding drag to the near-surface layers alone, and to the WA(*n*). We find that when drag is added uniformly to the near-surface environment, it is possible to extract kinetic energy at rates exceeding 428 TW, whereas when drag is added uniformly through-

out the entire atmosphere the lower bound exceeds 1,873 TW. The present total global power demand is ~ 18 TW (ref. 2).

We find that civilization-scale reliance on wind power, if uniformly distributed, might change zonal mean temperature by ~ 0.1 K and zonal mean precipitation by $\sim 1\%$. Consistent with previous literature, we find that large-scale near-surface KEE has a small surface warming effect, whereas whole-atmosphere KEE has a cooling effect. In both cases we observe a decrease in global average precipitation.

If the Earth were not rotating, atmospheric mass would accelerate down pressure gradients, rapidly converting available potential energy to kinetic energy. In contrast, on a rotating Earth with an atmosphere with zero viscosity, apparent Coriolis forces would balance pressure gradient forces and flows would be geostrophic (that is, along surfaces of constant pressure), with no conversion of potential to kinetic energy. Added drag forces cause atmospheric flows to depart further from geostrophy, and thus permit more rapid conversion of available potential energy to kinetic energy (see Supplementary Information). Increased net kinetic energy production can be sustained only by increased net production of available potential energy (APE). Increased production of APE results from increased diabatic heating of warm air masses or decreased diabatic heating of cool air masses. In our simulations, the area of snow- and ice-covered land expands as KEE increases. One source of increased production of APE in these simulations is the decreased diabatic heating over these newly snow- and ice-covered regions.

To obtain limits on the rate at which kinetic energy may be extracted from the atmosphere, we consider only the idealized cases in which drag is uniformly applied. We show that roughly equivalent amounts of KEE have different consequences for the Earth's climate and general circulation, depending on whether the extraction is confined to the near-surface or is applied throughout the whole atmosphere. This strongly suggests that our results would be different had we restricted this drag by applying it to high-velocity winds, to certain geographical regions or to specified vertical levels. Future work will investigate these cases, and will establish geophysical limits on wind power extraction in more realistic contexts. However, it seems that the future of wind energy will be determined by economic, political and technical constraints, rather than global geophysical limits.

Methods

All simulations were performed using the National Center for Atmospheric Research Community Atmosphere Model, Version 3.5 (CAM3.5) in a configuration with a mixed-layer ocean with specified ocean heat transport¹⁵. The model resolution was 2° in latitude by 2.5° in longitude with 26 levels in the vertical dimension. All simulations were integrated for 100 years. Simulations approach a stationary state on the timescale of decades; the final 60 years of each simulation were used for analysis.

A series of simulations (labelled SL(n)) were performed with drag added to the two lowest model layers, schematically representing ground-based wind turbines, with effective extraction areas per unit volume of atmosphere of $\rho_{\text{Area}} = 10^{-n} \text{ m}^{-1}$ for $n = \{5, 5.5, \dots, 8.5, 9\}$. Another series of simulations (labelled WA(n)) had drag forces applied throughout the whole atmosphere using the

same values of ρ_{Area} . Note that these simulations correspond to effective drag areas ranging from one square metre per cubic kilometre of model atmosphere (the $n = 9$ cases) to $10,000 \text{ m}^2 \text{ km}^{-3}$ ($n = 5$). Two further simulations were performed: a control run with $\rho_{\text{Area}} = 0$, and a simulation labelled WA(7.63) with effective drag area $23.4 \text{ m}^2 \text{ km}^{-3}$, designed to yield a global average KEE rate similar to the SL(5) case.

Received 1 May 2012; accepted 8 August 2012; published online 9 September 2012

References

1. Archer, C. & Caldeira, K. Global assessment of high-altitude wind power. *Energies* **2**, 307–319 (2009).
2. US Energy Information Administration. International energy statistics database. Accessed May 2012; available at www.eia.gov/ies.
3. Chen, G., Held, I. & Robinson, W. Sensitivity of the latitude of the surface westerlies to surface friction. *J. Atmos. Sci.* **64**, 2899–2915 (2007).
4. Keith, D. W. *et al.* The influence of large-scale wind power on global climate. *Proc. Natl Acad. Sci. USA* **101**, 16115–16120 (2004).
5. Wang, C. & Prinn, R. Potential climatic impacts and reliability of very large-scale wind farms. *Atmos. Chem. Phys.* **10**, 2053–2061 (2010).
6. Kirk-Davidoff, D. & Keith, D. On the climate impact of surface roughness anomalies. *J. Atmos. Sci.* **65**, 2215–2234 (2008).
7. Miller, L. M., Gans, F. & Kleidon, A. Estimating maximum global land surface wind power extractability and associated climatic consequences. *Earth Syst. Dynam.* **2**, 1–12 (2011).
8. Miller, L., Gans, F. & Kleidon, A. Jet stream wind power as a renewable energy resource: Little power, big impacts. *Earth Syst. Dynam.* **2**, 201–212 (2011).
9. Boville, B. & Bretherton, C. Heating and kinetic energy dissipation in the NCAR community atmosphere model. *J. Clim.* **16**, 3877–3887 (2003).
10. Zhou, L. *et al.* Impacts of wind farms on land surface temperature. *Nature Clim. Change* **2**, 539–543 (2012).
11. Hide, R. An experimental study of thermal convection in a rotating liquid. *Phil. Trans. R. Soc. Lond. A* **250**, 441–478 (1958).
12. Del Genio, A. & Suozzo, R. A comparative study of rapidly and slowly rotating dynamical regimes in a terrestrial general circulation model. *J. Atmos. Sci.* **44**, 973–986 (1987).
13. Navarra, A. & Boccaletti, G. Numerical general circulation experiments of sensitivity to earth rotation rate. *Clim. Dynam.* **19**, 467–483 (2002).
14. Hunt, B. The influence of the earth's rotation rate on the general circulation of the atmosphere. *J. Atmos. Sci.* **36**, 1392–1408 (1979).
15. Collins, W. *et al.* *Description of the NCAR Community Atmosphere Model (CAM 3.0)* Technical Report, (National Center for Atmospheric Research, 2004).

Acknowledgements

We wish to thank L. Cao for his help in configuring and running CAM and C. Doutriaux, P. Caldwell and K. Taylor for useful discussions. This work was performed under the auspices of the US Department of Energy by Lawrence Livermore National Laboratory under Contract DE-AC52-07NA27344.

Author contributions

K.M. and K.C. designed the study. K.M. prepared and performed the simulations. K.M., K.C. and B.K. analysed the data. K.M. and K.C. wrote the paper with contributions from B.K.

Additional information

Supplementary information is available in the online version of the paper. Reprints and permissions information is available online at www.nature.com/reprints. Correspondence and requests for materials should be addressed to K.M.

Competing financial interests

The authors declare no competing financial interests.